Acta Crystallographica Section F
Structural Biology and Crystallization Communications
ISSN 1744-3091

Crystallization and preliminary X-ray diffraction data of an LNA 7-mer duplex derived from a ricin aptamer

Charlotte Förster,[a] Dominik Oberthuer,[b] Jiang Gao,[a] André Eichert,[a] Frederick G. Quast,[a] Christian Betzel,[b] Andreas Nitsche,[c] Volker A. Erdmann[a] and Jens P. Fürste[a]*

[a]Institute of Chemistry and Biochemistry, Free University Berlin, Thielallee 63, 14195 Berlin, Germany, [b]Institute of Biochemistry and Food Chemistry, University of Hamburg, Notkestrasse 85, Building 22a, c/o DESY, 22603 Hamburg, Germany, and [c]Robert Koch-Institut, Zentrum für Biologische Sicherheit 1, Nordufer 20, 13353 Berlin, Germany

Correspondence e-mail: fuerste@chemie.fu-berlin.de

Received 19 June 2009
Accepted 22 July 2009

Locked nucleic acids (LNAs) are modified nucleic acids which contain a modified sugar such as β-D-2′-*O*,4′-*C* methylene-bridged ribofuranose or other sugar derivatives in LNA analogues. The β-D-2′-*O*,4′-*C* methylene ribofuranose LNAs in particular possess high stability and melting temperatures, which makes them of interest for stabilizing the structure of different nucleic acids. Aptamers, which are DNAs or RNAs targeted against specific ligands, are candidates for substitution with LNAs in order to increase their stability. A 7-mer helix derived from the terminal part of an aptamer that was targeted against ricin was chosen. The ricin aptamer originally consisted of natural RNA building blocks and showed high affinity in ricin binding. For future stabilization of the aptamer, the terminal helix has been constructed as an 'all-locked' LNA and was successfully crystallized in order to investigate its structural properties. Optimization of crystal growth succeeded by the use of different metal salts as additives, such as $CuCl_2$, $MgCl_2$, $MnCl_2$, $CaCl_2$, $CoCl_2$ and $ZnSO_4$. Preliminary X-ray diffraction data were collected and processed to 2.8 Å resolution. The LNA crystallized in space group $P6_5$, with unit-cell parameters $a = 50.11$, $b = 50.11$, $c = 40.72$ Å. The crystals contained one LNA helix per asymmetric unit with a Matthews coefficient of 3.17 Å^3 Da^{-1}, which implies a solvent content of 70.15%.

1. Introduction

Aptamers are nucleic acids which are selected for specific target binding from a large library by the recently developed 'SELEX' method ('systematic evolution of ligands by exponential enrichment'; Ellington & Szostak, 1990; Tuerk & Gold, 1990). The aptamers bind the targets against which they are selected with high affinity and selectivity, similar to the function of an antibody. However, aptamers are much smaller in molecular mass than antibodies, which mostly lie in the range 10–15 kDa (White *et al.*, 2000). The therapeutical and diagnostic potential of aptamers, as well as the binding properties of aptamers to their ligands, have been investigated thoroughly and reviewed extensively (Hermann & Patel, 2000; Nimjee *et al.*, 2005; Rimmele, 2003; Tombelli *et al.*, 2005).

The first aptamer drug and the best example of their therapeutical potential is the aptamer drug macugen, which acts as an endothelial growth-factor antagonist in the therapy of neurovascular age-dependent macular degeneration (Gryziewicz, 2005). Another example is provided by the tenascin C-related tumour-marker aptamer, which is undergoing clinical trials (Schmidt *et al.*, 2004). The selectivity and binding specificity of aptamers which were developed against D-adenosine or against L-arginine have been demonstrated in our laboratory (Klussmann *et al.*, 1996; Nolte *et al.*, 1996). In general, aptamers show low or no immunogenicity and can in principle be developed against arbitrary ligands; these facts open a broad field of possible applications in diagnostic and therapeutic medicine.

Great interest is focused on the stabilization of aptamer tertiary structures. A high *in vitro* stability for nucleic acids in general has been achieved by the introduction of locked nucleic acid building

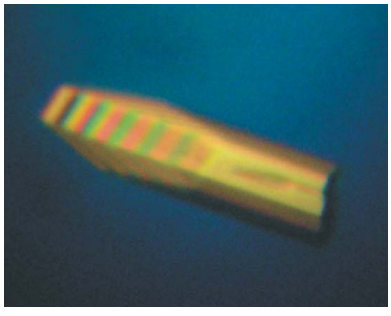

blocks (LNAs), which were first synthesized in the institutes of T. Imanishi (Obika *et al.*, 1997) and J. Wengel (Kumar *et al.*, 1998). The 'LNA family' consists of chemically synthesized nucleic acids with modified sugar moieties, such as *β*-D-2′-*O*,4′-*C* methylene cross-linked ribofuranose. It has been generally proven that LNAs show increased stability with respect to their melting behaviour, as could also be demonstrated for the tenascin C-binding aptamer TTA-1 after substitution with different modified nucleic acid blocks. With respect to the thermal *in vitro* stability, the following order could be observed for the melting temperature of the aptamer: 2′-F/2′-OMe < RNA/RNA ≤ 2′-OMe/2′-OMe < 2′-F/LNA < RNA/LNA < 2′-OMe/LNA < LNA/LNA (Schmidt *et al.*, 2004). Enhanced thermostability in LNA-substituted nucleic acids has been demonstrated in the laboratories of P. Jacobsen and J. Wengel (Petersen *et al.*, 2000). The studies showed that the *β*-D-2′-*O*,4′-*C* methylene ribofuranose 'locks' the LNA in the C3′-*endo* conformation, which influences the geometry of the phosphate backbone and orients the duplex in a manner that produces more efficient base stacking (Obika *et al.*, 1997; Petersen & Wengel, 2003). Intensive structural studies have been performed using heteroduplexes such as *β*-D- or *α*-L-LNA/DNA mix-mers hybridized to RNA or DNA. *β*-D-LNA (LNA/DNA mix-mer)–RNA duplexes adopt the A-type conformation, whereas *α*-L-LNA (LNA/DNA mix-mer)–DNA helices adopt the B-type conformation (Petersen *et al.*, 2002; Vester & Wengel, 2004). The NMR structures of a fully modified LNA hybridized to RNA or DNA showed the following: generally, *β*-D-LNA introduces the A-type nucleic acid conformation into the duplexes, with the conformation in the *β*-D-LNA–DNA duplex being an equilibrium between N- and S-type sugar puckers (Nielsen *et al.*, 2004).

Here, we focus our interest on the RNA-based ricin aptamer which was recently developed by Ellington and coworkers (Hesselberth *et al.*, 2000). A shortened aptamer named RA80.1.d1 (Fig. 1) was shown to be fully biologically active. As we are generally interested in the stabilization of different aptamers, we decided to take the anti-ricin aptamer as a model substance for substitution with *β*-D-2′-*O*,4′-*C* methylene ribofuranose locked nucleic acids. We chose the terminal stem of the RNA aptamer, which is indicated in Fig. 1, and it was constructed as an 'all-locked' 7-mer duplex. By comparative crystallization and X-ray structure analysis of the 'all-LNA' duplex and the RNA counterpart, we hope to provide a basic structural comparison between the two helices which might help in investigating the enhanced thermostability in LNA-substituted nucleic acids.

Figure 1
The sequence of the RA80.1.d1 ricin aptamer derived from Hesselberth *et al.* (2000). The box indicates the stem region which was designed as 'all-locked' nucleic acid and investigated by X ray diffraction analysis.

2. Materials and methods

2.1. Crystallization of the 7-mer LNA helix and measurement of melting curves

The sequence of the LNA helix was derived from the terminal part of the ricin aptamer, which was developed as an RNA molecule (Hesselberth *et al.*, 2000). The 7-mer helix in this study was designed as an all-LNA and consists of nucleotide building blocks which contain the *β*-D-2′-*O*,4′-*C* methylene modified ribofuranose instead of the natural ribose. Chemically synthesized nucleic acid oligonucleotides with sequences 5′-LNT-LNG-LNG-LNA-LNT-LNC-LNC-3′ and 5′-LNG-LNG-LNG-LNT-LNT-LNC-LNA-3′ were purchased from IBA (Göttingen, Germany) and were purified by HPLC by the company. Both LNA strands were annealed in distilled water at a concentration of 0.1 m*M*. The strands were combined and heated to 363 K for 5 min and subsequently cooled to room temperature for several hours. The resulting LNA duplex was concentrated to 0.5 m*M* in a speed vac (SpeedVac SC 110, Savant, Minnesota, USA) and used in all subsequent crystallization experiments. For the measurement of the melting curves of LNA *versus* RNA, RNA 7-mer oligonucleotides with corresponding sequences were purchased from IBA (Göttingen, Germany). The LNAs and RNAs were annealed and concentrated as described above for the LNA crystallization experiments, while the final concentration used for measuring the melting curves was 5.0 µ*M*.

Initially, two different nucleic acid screening kits were used for crystallization experiments. At first, the Natrix Nucleic Acid Crystallization Kit (HR2-116; Hampton Research, California, USA), which contains 48 different crystallization conditions, was used by applying the sitting-drop vapour-diffusion technique with CrystalQuick Lp plates from Greiner Bio-One (Germany). 1 µl of a 0.5 m*M* LNA solution in distilled water was mixed with 1 µl reservoir solution and equilibrated against 80 µl reservoir solution at 294 K. Secondly, the Nucleic Acid Mini Screen from Hampton Research (HR2-118) with 24 different conditions was applied using the hanging-drop vapour-diffusion technique and Linbro Plates (ICN Biomedicals Inc., Aurora, Ohio, USA). In this experiment, 1 µl of the 0.5 m*M* aqueous LNA solution was mixed with 1 µl crystallization solution from the screen and equilibrated against 1 ml reservoir solution which contained 35%(*v*/*v*) 2-methyl-2,4-pentanediol (MPD) in distilled water pH 7.4 at a temperature of 294 K.

Crystal optimization was performed using the hanging-drop vapour-diffusion technique in Linbro Plates (ICN Biomedicals Inc.) as described above. The basic conditions consisted of 50 m*M* sodium cacodylate pH 6.0, 1.0 *M* lithium sulfate and 10 m*M* $MgCl_2$. The exchange of $MgCl_2$ for $CuCl_2$, $MnCl_2$, $CaCl_2$, $CoCl_2$ or $ZnSO_4$ led to the final successful crystallization. The best crystal growth was achieved using $ZnSO_4$ as an additive instead of $MgCl_2$.

In order to investigate the thermostability of the LNA compared with the RNA duplex, we measured the melting curves of both the LNA and RNA 7-mer helices. The melting curves were recorded on a Hewlett Packard 8452A Diode Array spectrophotometer in 1.73 m*M* disodium hydrogen phosphate, 1 m*M* potassium dihydrogen phosphate pH 7.2, 100 m*M* sodium chloride and 0.1 m*M* EDTA using a concentration of 5.0 µ*M* RNA or LNA. The OD_{260} was measured as a function of temperature within the range 283–363 K with steps of 1 K

increase per minute. The T_m values were obtained from the maxima of the first derivatives of the melting curves.

2.2. Acquisition of the X-ray diffraction data and data processing

Prior to X-ray diffraction data collection, the crystals were flash-frozen in a cryoprotectant solution containing 50 m*M* sodium cacodylate pH 6.0, 1 *M* lithium sulfate, 10 m*M* of the corresponding salt listed above and 20%(*v*/*v*) glycerol.

The X-ray diffraction data were recorded on the DESY Synchrotron (Hamburg, Germany) consortium beamline X13 at a wavelength of 0.8123 Å. A data set was recorded from 50 to 2.3 Å resolution at a temperature of 100 K. The crystallographic data were analyzed and processed to 2.8 Å resolution using programs from the *HKL*-2000 suite (Otwinowski & Minor, 1997). The solvent content of the crystals was calculated by the method of Voss & Gerstein (2005), considering the standard atomic values for RNA, assuming that the LNA packing may be comparable with that of RNA.

To check for twinning, which is of common occurrence in RNA crystals in our experience, the data sets were analyzed using the Padilla and Yeates algorithm (Padilla & Yeates, 2003) as implemented by the web server http://nihserver.mbi.ucla.edu/pystats. The LNA data set showed a curve which corresponded to a theoretically untwinned crystal, so we have no indication of merohedral twinning.

At present, molecular-replacement calculations are in progress using an artificial LNA helix. The basis for the model was an LNA duplex 7-mer structure that has been solved recently (unpublished results) in which the sequence has been adapted to that of the present LNA duplex from the ricin aptamer. The sugars in the model corresponded to the LNA modifications; they were constructed as β-D-2′-*O*,4′-*C* methylene-bridged ribofuranoses. The program *Phaser* (Read & Schierbeek, 1988) was used for the initial MR calculations and *REFMAC*5 (Murshudov *et al.*, 1997) was used for initial structure refinement. Both programs were used as implemented in the *CCP*4*i* package (Collaborative Computational Project, Number 4, 1994). *Coot* was used for model building (Emsley & Cowtan, 2004).

3. Results and discussion

3.1. Crystallization

We are interested in the stabilization of aptamers by introducing modified nucleic acids into the stem regions. As the order of thermostability for modified nucleic acids is described to be 2′-F/2′-OMe <

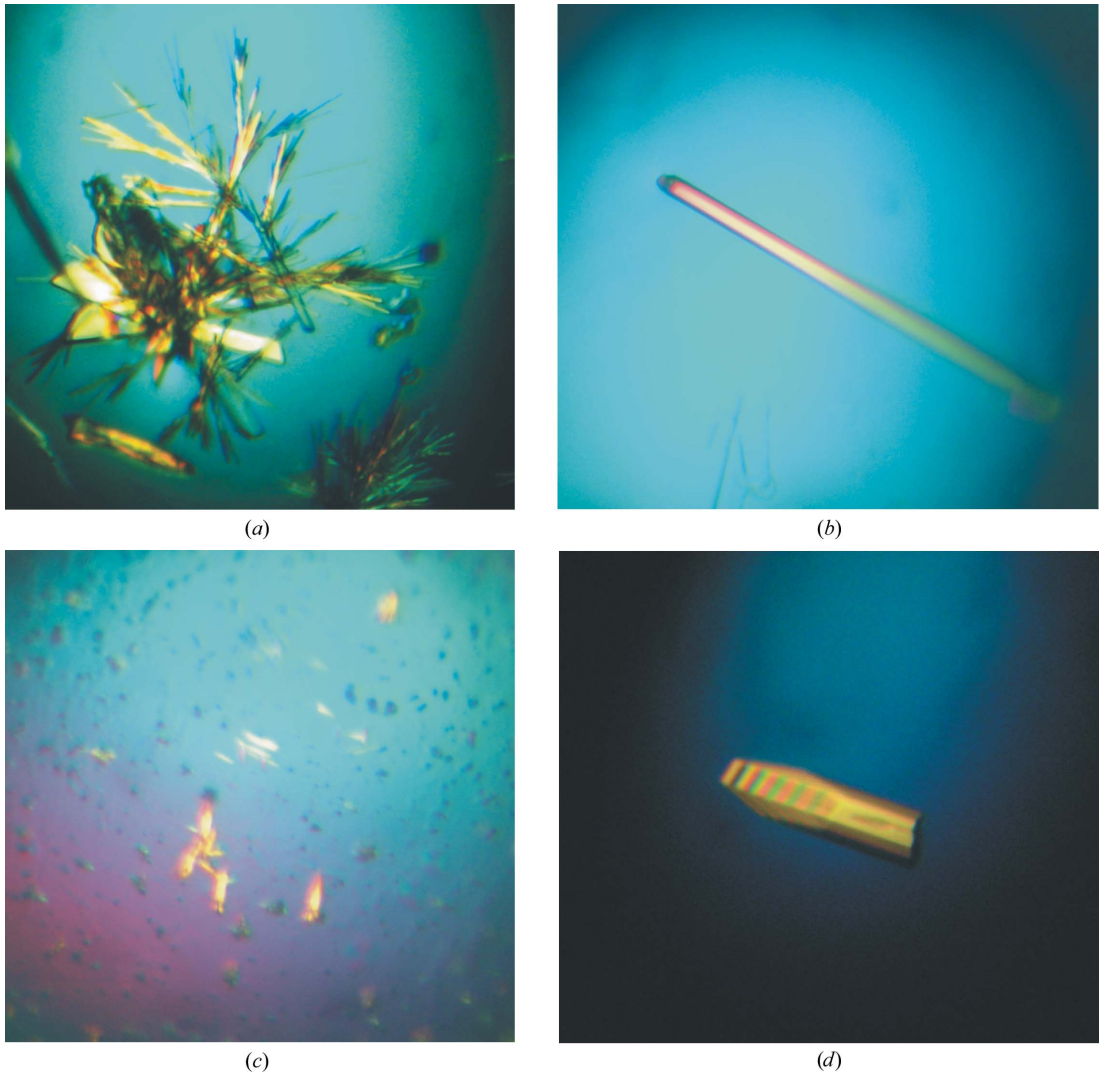

Figure 2
Optimization of LNA crystal growth using different metal salts as an additive: (*a*) 10 m*M* $MgCl_2$, (*b*) 10 m*M* $CaCl_2$, (*c*) 10 m*M* $CuCl_2$, (*d*) 10 m*M* $ZnSO_4$. The basic conditions in all setups consisted of 50 m*M* sodium cacodylate pH 6.0 and 1 *M* lithium sulfate. The crystals in (*d*) had approximate dimensions of 0.25 × 0.25 × 0.8 mm.

RNA/RNA ≤ 2′-OMe/2′-OMe < 2′-F/LNA < RNA/LNA < 2′-OMe/LNA < LNA/LNA (Schmidt *et al.*, 2004), we focused on introducing LNA helices into the aptamer structures. As a first model, we designed a stem region originating from the ricin aptamer (Hesselberth *et al.*, 2000) as an 'all-locked' 7-mer β-D-2′-*O*,4′-*C* methylene ribofuranose LNA which contains exclusively locked nucleic acid building blocks.

The LNA duplex (Fig. 1) initially crystallized in 50 m*M* sodium cacodylate pH 6.0, 10 m*M* magnesium chloride, 1.0 *M* lithium sulfate at 294 K after a few days. The small crystals had no clear morphology and optimization of the precipitant and temperature was not successful. By exchanging 10 m*M* $MgCl_2$ for 10 m*M* $MnCl_2$ or $CaCl_2$, the crystal morphology and size could be reproducibly influenced to a great extent (Figs. 2*a* and 2*b*). This observation led to the idea to further exchange the metal ion by using other heavy-metal salts as additives. We further cocrystallized the LNA duplex with $CuCl_2$, $CoCl_2$, $NiCl_2$ or $ZnSO_4$ (Figs. 2*c* and 2*d*) and observed a large influence on crystal growth and crystal morphology depending on the metal ion added in the setups. The best crystals were obtained with $ZnSO_4$ as an additive, with the final conditions being 50 m*M* sodium cacodylate pH 6.0, 10 m*M* $ZnSO_4$ and 1.0 *M* lithium sulfate at a temperature of 294 K. The crystals appeared after several days and had approximate dimensions of 0.25 × 0.25 × 0.8 mm (Fig. 2*d*).

3.2. Crystallographic data and T_m values

The 7-mer 'all-LNA' duplex crystallized in space group $P6_5$, with one molecule in the asymmetric unit. The crystals with the best morphology, which were grown using $ZnSO_4$ as an additive, corresponded to the crystals with the best crystallographic data; all other crystals gave poor diffraction. A data set for the LNA crystal with $ZnSO_4$ was acquired in the resolution range 50–2.3 Å on the DESY consortium beamline X13 (Hamburg, Germany) and the data were processed to 2.8 Å resolution. The crystallographic parameters of the all-LNA ricin-aptamer helix are listed in Table 1. From our data set, we calculated a Matthews coefficient of 3.17 Å^3 Da^{-1} with one LNA helix per asymmetric unit (Matthews, 1968). The solvent content of 70.2% seems high, but we have often observed solvent contents of approximately 65–66% for RNA crystals (Förster, Brauer *et al.*, 2007; Förster, Perbandt *et al.*, 2007). We can exclude the presence of a second LNA helix in the asymmetric unit as this would imply a Matthews coefficient of 1.58 Å^3 Da^{-1} and a solvent content of 40.1%.

Table 1
Data-collection and processing statistics for the 'all-LNA' duplex originating from the ricin aptamer RA80.1.d1 (Hesselberth *et al.*, 2000).

The data correspond to the crystal grown with $ZnSO_4$ as an additive; details are described in the text. Values in parentheses are for the highest resolution shell.

Beamline	DESY consortium beamline X13
Wavelength (Å)	0.8123
Space group	$P6_5$
Unit-cell parameters (Å)	a = 50.11, b = 50.11, c = 40.23
Matthews coefficient V_M (Å^3 Da^{-1})	3.17
LNA duplexes per ASU	1
Solvent content† (%)	70.15
Measured reflections	5223
Unique reflections	1371
Resolution range (Å)	50.0–2.80 (2.85–2.80)
Completeness (%)	93.1 (100.0)
Multiplicity	3.8 (4.0)
R_{merge}‡ (%)	5.1 (14.5)
Average $I/\sigma(I)$	18.0 (1.2)

† As calculated using the method of Voss & Gerstein (2005). ‡ $R_{merge} = \sum_{hkl}\sum_i |I_i(hkl) - \langle I(hkl)\rangle| / \sum_{hkl}\sum_i I_i(hkl)$, where $I_i(hkl)$ and $\langle I(hkl)\rangle$ are the observed individual and mean intensities of a reflection with indices *hkl*, respectively, $\sum_i$ is the sum over the individual measurements of a reflection with indices *hkl* and $\sum_{hkl}$ is the sum over all reflections.

Therefore, the crystals possess packing parameters with a relatively high solvent content.

A possible structure solution of the LNA duplex was found by molecular replacement using an artificial LNA as a model. A comparison of the β-D-2′-*O*,4′-*C* methylene ribofuranose moiety of the LNA with the natural ribose is shown in Fig. 3. Within the molecular-replacement calculation, the translation function gave a *Z* score of 7.0 and the rotation function gave a *Z* score of 3.6. After initial refinement calculations and the addition of solvent molecules, the *R* values fell from R/R_{free} = 50.3/48.9% to values in the region of R/R_{free} = 30/34%. It was on the basis of this likely structure solution that we assigned the space group as $P6_5$. The nucleotide structures in Fig. 3 are taken from an X-ray structure analysis of a tRNA^{Ser} microhelix, comparing that microhelix designed as RNA (Eichert *et al.*, 2009) with a preliminary one designed as LNA (unpublished results) in our laboratory. The nucleic acid libraries in *REFMAC* (Murshudov *et al.*, 1997) consisted of either the standard RNA or LNA descriptions. The nucleotides in Fig. 3 provide a basic comparison between RNA and LNA and show the β-D-2′-*O*,4′-*C* methylene cross-linked ribofuranose in LNAs.

Further refinement does not improve the *R* values at present and we will therefore have to focus on improving the crystal quality. We

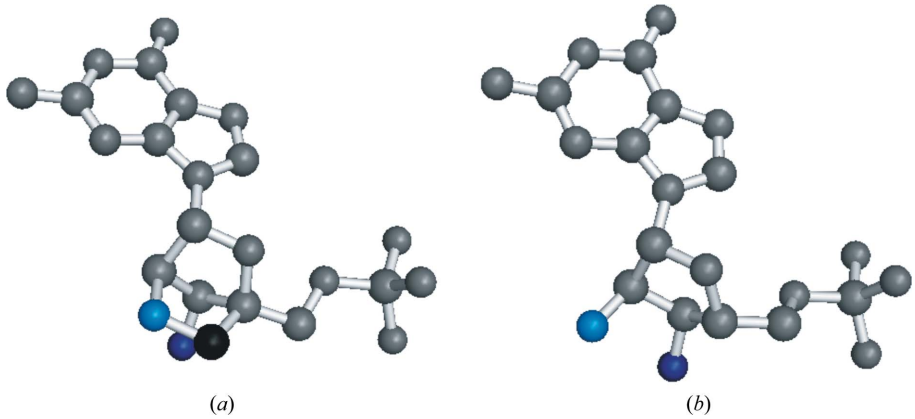

(*a*) (*b*)

Figure 3
The sugar moiety of the LNA helix investigated here is the β-D-2′-*O*,4′-*C* methylene-bridged ribofuranose (*a*; the C atom of the methylene bridge is highlighted in black) and is compared here with the natural ribose in RNA (*b*). The 2′ and 3′ sugar O atoms are marked in light blue and dark blue, respectively. Details of the origins of the nucleotides are described in the text.

have noticed that the crystals are extremely sensitive to soaking in cryoprotecting solution and to transportation. Immediate freezing of the crystals in liquid nitrogen directly after their appearance might help to further improve the quality of the X-ray diffraction data and to calculate the final structure. Also, the addition of other metal ions may further improve the crystal quality.

We measured the T_m values of the LNA duplex and the corresponding RNA duplex to investigate the thermostability of the helices. As described above, LNAs possess enhanced stability compared with the unmodified RNA molecules. The LNA duplex investigated here shows a T_m value of 357.4 K, whereas the RNA with the corresponding sequence gives a value of T_m = 295.5 K.

With this work, we wish to contribute to the basic chemical understanding of the enhanced thermostability of locked nucleic acids. The crystal structure of an 'all-locked' β-D-2′-*O*,4′-*C* methylene ribofuranose LNA helix will contribute to the general understanding of LNA conformation and stability. Additionally, we are highly interested in techniques involving the application of LNAs. One objective is the insertion of LNA duplexes into the stem regions of aptamers that are designed against bioterrorism reagents such as ricin, anthrax, vaccinia virus or botox. The introduction of LNA stem regions should increase the stability of aptamers to a great extent by leaving the biologically active RNA or DNA loop regions that interact with the ligands unaffected. There are several reports in the literature that describe the biological activity of LNA-substituted nucleic acids. One example is the use of LNA modifications within hammerhead ribozymes that improve the cleavage reaction (Christiansen *et al.*, 2007). Another study involves the introduction of LNAs into antisense oligonucleotides and DNAzymes that are targeted to functionally selected binding sites and inhibit HIV-1 expression (Jakobsen *et al.*, 2007). LNAs have also been introduced into the G-quadruplex thrombin aptamer, which retained its biological activity to different extents depending on the nucleotide positions that were modified (Bonifacio *et al.*, 2008). These and other reports encourage us to believe that the introduction of an LNA stem into the ricin aptamer might not affect its function and that the ricin-binding capacity might be maintained. At present, investigations are in progress to examine the biological activity of the ricin aptamer after introduction of LNA modifications into the stem region.

This work was supported within the BMBF/VDI-financed BiGRUDI network of the Robert Koch Institute (Berlin). We gratefully acknowledge the DESY synchrotron facility, Hamburg, Germany for providing beam time and Ursula Erikli for copy-editing the manuscript.

References

Bonifacio, L., Church, F. C. & Jarstfer, M. B. (2008). *Int. J. Mol. Sci.* **9**, 422–433.
Christiansen, J. K., Lobedanz, S., Arar, K., Wengel, J. & Vester, B. (2007). *Bioorg. Med. Chem.* **15**, 6135–6143.
Collaborative Computational Project, Number 4 (1994). *Acta Cryst.* D**50**, 760–763.
Eichert, A., Fürste, J. P., Schreiber, A., Perbandt, M., Betzel, C., Erdmann, V. A. & Förster, C. (2009). *Biochem. Biophys. Res. Commun.* **386**, 368–373.
Ellington, A. D. & Szostak, J. W. (1990). *Nature (London)*, **346**, 818–822.
Emsley, P. & Cowtan, K. (2004). *Acta Cryst.* D**60**, 2126–2132.
Förster, C., Brauer, A. B. E., Lehmann, D., Borowski, T., Brode, S., Fürste, J. P., Perbandt, M., Betzel, C. & Erdmann, V. A. (2007). *Acta Cryst.* F**63**, 839–843.
Förster, C., Perbandt, M., Brauer, A. B. E., Brode, S., Fürste, J. P., Betzel, C. & Erdmann, V. A. (2007). *Acta Cryst.* F**63**, 46–48.
Gryziewicz, L. (2005). *Adv. Drug Deliv. Rev.* **57**, 2092–2098.
Hermann, T. & Patel, D. J. (2000). *Science*, **287**, 820–825.
Hesselberth, J. R., Miller, D., Robertus, J. & Ellington, A. D. (2000). *J. Biol. Chem.* **275**, 4937–4942.
Jakobsen, M. R., Haasnoot, J., Wengel, J., Berkhout, B. & Kjems, J. (2007). *Retrovirology*, **4**, 29.
Klussmann, S., Nolte, A., Bald, R., Erdmann, V. A. & Fürste, J. P. (1996). *Nature Biotechnol.* **14**, 1112–1115.
Kumar, R., Singh, S. K., Koshkin, A. A., Rajwanshi, V. K., Meldgaard, M. & Wengel, J. (1998). *Bioorg. Med. Chem. Lett.* **8**, 2219–2222.
Matthews, B. W. (1968). *J. Mol. Biol.* **33**, 491–497.
Murshudov, G. N., Vagin, A. A. & Dodson, E. J. (1997). *Acta Cryst.* D**53**, 240–255.
Nielsen, K. E., Rasmussen, J., Kumar, R., Wengel, J., Jacobsen, J. P. & Petersen, M. (2004). *Bioconjug. Chem.* **15**, 449–457.
Nimjee, S. M., Rusconi, C. P. & Sullenger, B. A. (2005). *Annu. Rev. Med.* **56**, 555–583.
Nolte, A., Klussmann, S., Bald, R., Erdmann, V. A. & Fürste, J. P. (1996). *Nature Biotechnol.* **14**, 1116–1119.
Obika, S., Nanbu, D., Hari, Y., Morio, K.-I., In, Y., Ishida, T. & Imanishi, T. (1997). *Tetrahedron Lett.* **38**, 8735–8738.
Otwinowski, Z. & Minor, W. (1997). *Methods Enzymol.* **276**, 307–326.
Padilla, J. E. & Yeates, T. O. (2003). *Acta Cryst.* D**59**, 1124–1130.
Petersen, M., Bondensgaard, K., Wengel, J. & Jacobsen, J. P. (2002). *J. Am. Chem. Soc.* **124**, 5974–5982.
Petersen, M., Nielsen, C. B., Nielsen, K. E., Jensen, G. A., Bondensgaard, K., Singh, S. K., Rajwanshi, V. K., Koshkin, A. A., Dahl, B. M., Wengel, J. & Jacobsen, J. P. (2000). *J. Mol. Recognit.* **13**, 44–53.
Petersen, M. & Wengel, J. (2003). *Trends Biotechnol.* **21**, 74–81.
Read, R. J. & Schierbeek, A. J. (1988). *J. Appl. Cryst.* **21**, 490–495.
Rimmele, M. (2003). *Chembiochem*, **4**, 963–971.
Schmidt, K. S., Borkowski, S., Kurreck, J., Stephens, A. W., Bald, R., Hecht, M., Friebe, M., Dinkelborg, L. & Erdmann, V. A. (2004). *Nucleic Acids Res.* **32**, 5757–5765.
Tombelli, S., Minunni, M. & Mascini, M. (2005). *Biosens. Bioelectron.* **20**, 2424–2434.
Tuerk, C. & Gold, L. (1990). *Science*, **249**, 505–510.
Vester, B. & Wengel, J. (2004). *Biochemistry*, **43**, 13233–13241.
Voss, N. R. & Gerstein, M. (2005). *J. Mol. Biol.* **346**, 477–492.
White, R. R., Sullenger, B. A. & Rusconi, C. P. (2000). *J. Clin. Invest.* **106**, 929–934.